Supplementary Information

Access to side-chain carbon information in deuterated solids under ultra-fast MAS through non-rotor-synchronized mixing

Natalia Kulminskaya[(a)#], Suresh Kumar Vasa[(a)#], Karin Giller[(a)], Stefan Becker[(a)], Ann Kwan[(b)], Margaret Sunde[(b)], Rasmus Linser[(a)*]

[(a)]Department of NMR-based Structural Biology, Max Planck Institute for Biophysical Chemistry, 37077 Göttingen, Germany
[(b)]School of Medical Sciences and School of Molecular Bioscience, University of Sydney, Sydney, Australia

Materials and methods

Sample preparation

SH3 domain of α-spectrin was prepared as described elsewhere.[1] A 100% ^{1}H back substitution of amide protons was used in conjunction with a fully ^{2}H, ^{13}C and ^{15}N-labeled protein. This protein preparation also contained CH_3 labeling at methyl sites of leucine, isoleucine, and valine, which was obtained upon additional use of 75 mg α-keto-isovalerate and 125 mg α-keto-butyrate as described previously for solution NMR.[1] Cu^{II} paramagnetic doping was utilized as reported previously using 75 mM $[Cu^{II}(edta)]^{2-}$.[2] For the NMR measurements, approximately 1 mg of the protein was transferred and centered in a 1.3-mm rotor. The sample preparation of $EAS_{\Delta 15}$ hydrophobin rodlets with 100% back exchanged amide protons has been described previously.[3] The protein was packed into the rotor after incubation of the rodlets in 75 mM $[Cu^{II}(edta)]^{2-}$ solution for 3-4 hours.

ssNMR experiments and analysis

All NMR experiments were performed on a Bruker Avance II NMR spectrometer with a ^{1}H Larmor frequency of 800 MHz equipped with a 1.3-mm HCN triple-resonance MAS probe. Experiments were recorded at an effective sample temperature of 303 K for both samples. All spectra were recorded at 55.5 kHz spinning speed, and 4,4-dimethyl-4-silapentane-1-sulfonic acid (DSS) was used as a standard for chemical shift referencing and temperature calibration. The variation in the spinning speed under these conditions is around ± 30 Hz. 90° hard pulses of 2.75 µs (91 kHz), 4.2 µs (59.5 kHz) and 6.6 µs (38 kHz) were applied on ^{1}H and ^{13}C and ^{15}N channels, respectively. For Hartmann-Hahn CP, the double-quantum (n = +1) condition was used with rf field strengths of 20.2 kHz and 54.1 kHz on the ^{1}H and ^{13}C channel, respectively, with a 100 – 90 % ramped CP pulse on the ^{1}H channel. The ^{1}H-^{13}C CP contact time was set to 2100 µs. For the ^{15}N-^{13}C CP the rf power was set to 36.7 kHz and 24.4 kHz on ^{13}C and ^{15}N channels, respectively, with a contact time of 9 ms. For the ^{15}N-^{1}H CP, power levels of 54.23 kHz and 14.4 kHz were used with a contact time of 300 µs. For the comparison experiments of MOCCA and RFDR, these parameters were kept constant. The B_1 field of the 180° pulses for MOCCA and RFDR was 59.5 kHz with a duration of the single 180° pulses of 8.37 µs. 2D ^{13}C-^{13}C MOCCA correlation spectra were acquired with spectral widths of 355 and 200 ppm in the direct and indirect dimensions, respectively, with total acquisition times of 15 ms and

8 ms. RFDR spectra were recorded using the same parameters, the only exception being the duration between the pulses, which was chosen in accordance with the rotor frequency. Unless otherwise stated, all MOCCA and RFDR experiments were recorded in 3 hours each. The estimated T_1 relaxation times on ^{13}C were ~1.8 s and ~0.8 s for hydrophobin and SH3 samples respectively. Two 3D CCCANH spectra were acquired for side-chain assignments of the SH3 and hydrophobin proteins, using two blocks of isotropic MOCCA mixing (Figure 1B). The 3D spectrum for SH3 was performed with a spectral width of 30 ppm (2640 points) in the direct (^{1}H) dimension and 32 ppm and 80 increments and 80 ppm and 256 increments in first (^{15}N) and second (^{13}C) indirect dimensions, respectively, using 8 scans. For the hydrophobin sample, a spectral width of 30 ppm and 2560 points in the direct (^{1}H) dimension and 32.7 ppm and 62 increments (^{15}N) and 138 ppm and 380 increments (^{13}C) in the indirect dimensions were used. All NMR data were processed using TopSpin 3.2 software and subsequently analyzed using Sparky.[4]

In the previous study, using 2D spectra we found optimal delay times of 60 µs and 100 µs to provide efficient transfer at low spinning speeds. Under fast MAS conditions, the delay was optimized using a set of 2D ^{13}C-^{13}C correlation experiments (Figure 2A). The delay between the 180° pulses was varied around 60 µs. Some extracted cross-peak intensities are depicted in Figure 2B and Figure S1. The maximum in peak intensity was found to be obtainable with 61.5 µs as the most suitable delay, 62 µs being the second best value determined (marked as dark and light green respectively, in both figures). A delay Δ of 61.5 µs and duration of the 180-degree pulse of 8.37 µs was further used for 2D and 3D experiments.

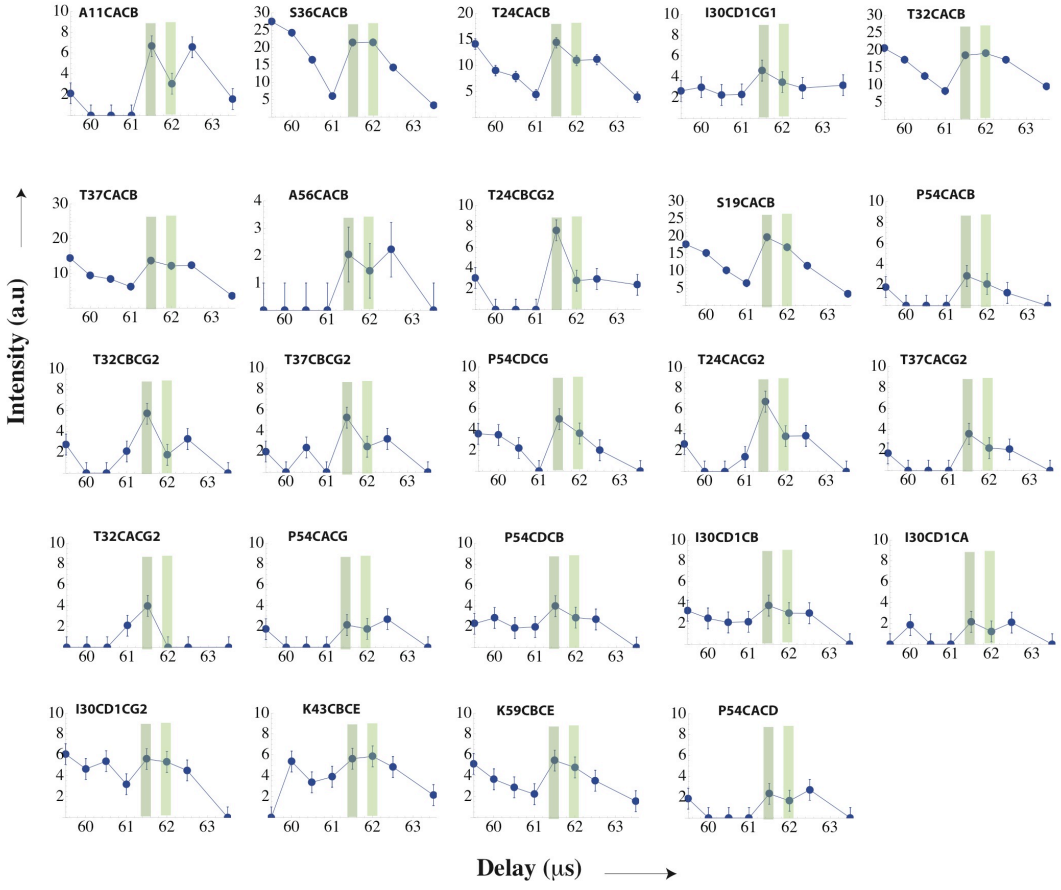

Fig. S1. Build up curves showing the experimental optimization of hard-pulse MOCCA, in addition to the peaks shown in the Main Text Figure 2B. The figure depicts different cross-peak intensities upon variation of global delay Δ. The total mixing time in all experiments was set to 35 ms. Suitable transfer efficiency conditions are shown in dark (and light) green colors.

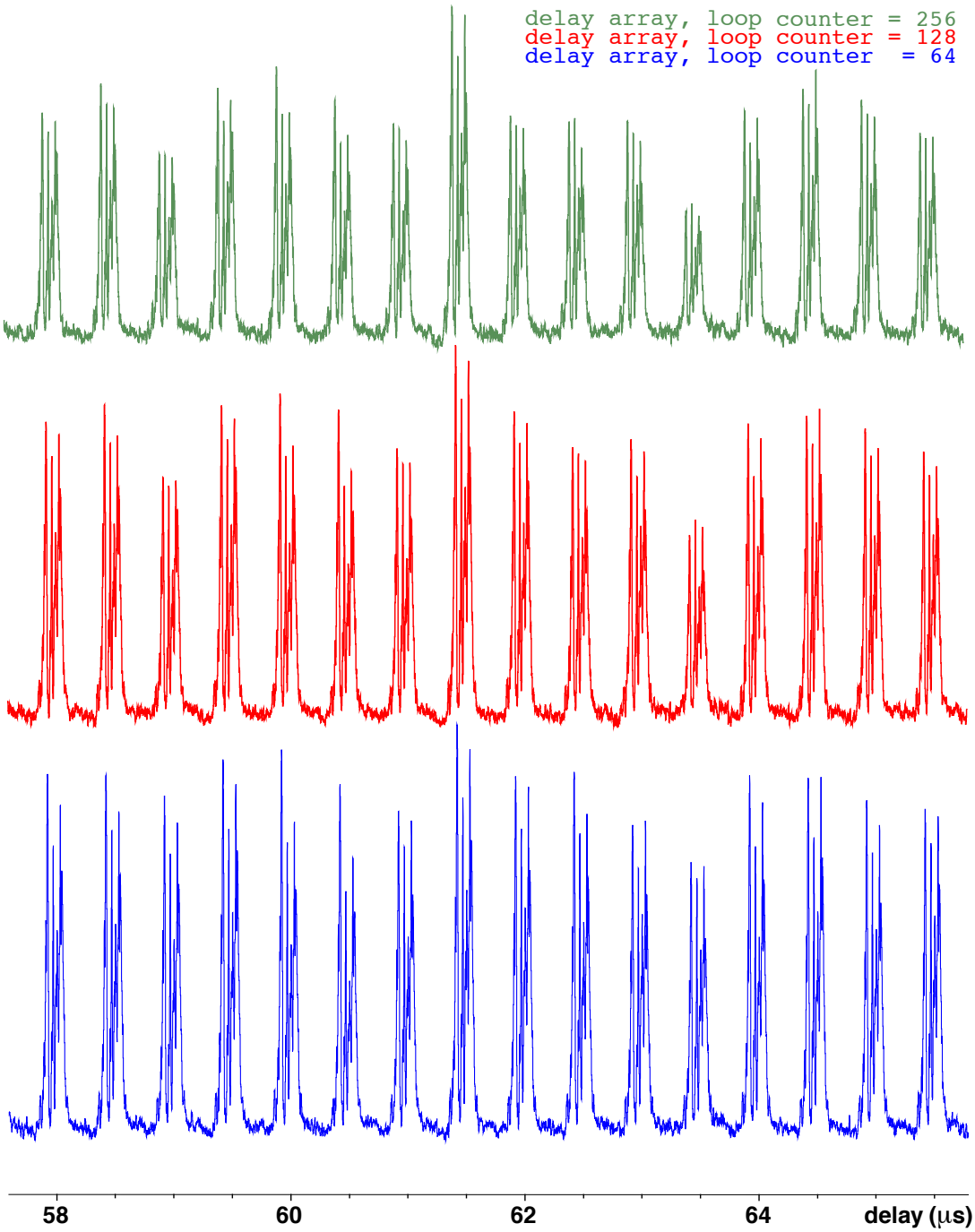

Fig. S2. Experimental optimization of the delay of MOCCA using only the bulk carbon magnetization. Corresponding mixing times for the loop counters are: 4.4 ms (in blue), 8.8 ms (red) and 17.5 ms (in green). The global optimum for all three representative plots is 61.5 ms. The data were obtained on an 800 MHz spectrometer at 55 kHz MAS for the SH3 domain.

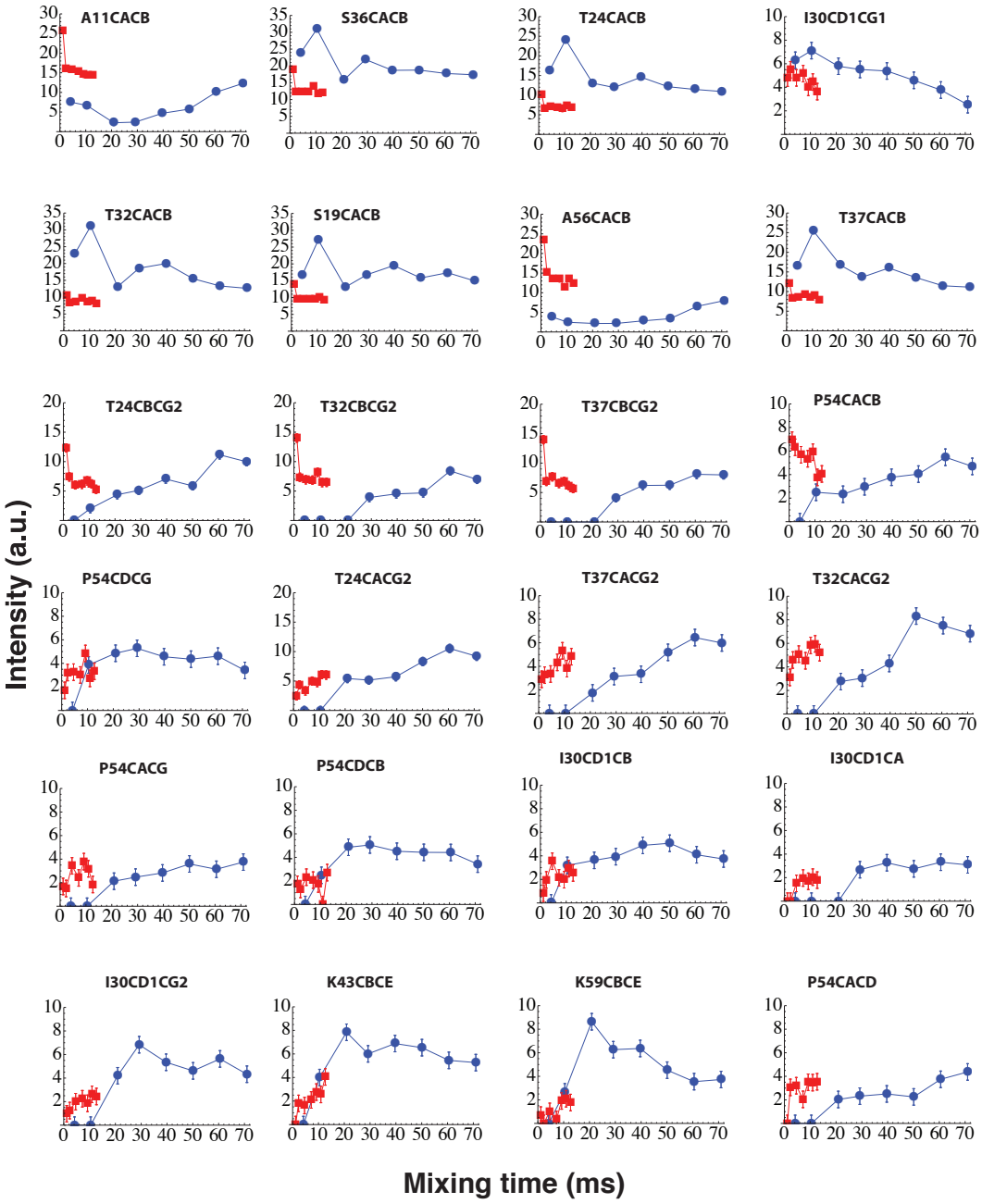

Fig. S3. ^{13}C-^{13}C transfer efficiency of MOCCA (blue spheres) and RFDR (red squares) as a function of mixing time. A series of 2D ^{13}C-^{13}C spectra was recorded on the SH3 domain with different isotropic mixing periods. The signal intensity for one-, two-, and three-bond magnetization transfer is plotted as a function of the ^{13}C-^{13}C mixing time. The RF pulse amplitude during carbon-carbon mixing times for both MOCCA and RFDR was set to 65 kHz. The delay in MOCCA hard pulse was set to 61.5 µs. For this comparison processing parameters were kept identical. Even if (in the hypothetical case that heating did not happen) RFDR mixing could be extended to a similar duration of mixing as MOCCA, this would mean a multitude of strong pulses. Consequently, due to pulse imperfections and rf inhomogeneity, for multiple-bond transfer we would still expect better performance of MOCCA.

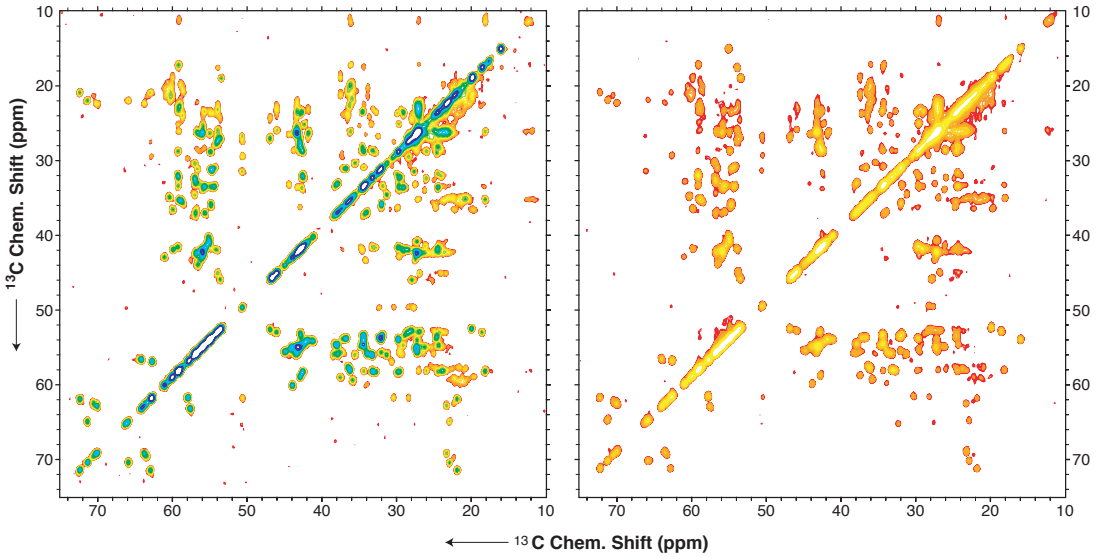

Fig. S4. 2D ^{13}C-^{13}C correlation spectra of [100% back exchanged 2D, 13C, 15N]- labeled SH3 protein with MOCCA (left, total mixing of 35 ms) and RFDR mixing (right, total mixing of 10 ms) at 55.5 kHz MAS. Each spectrum was recorded for 3 hours.

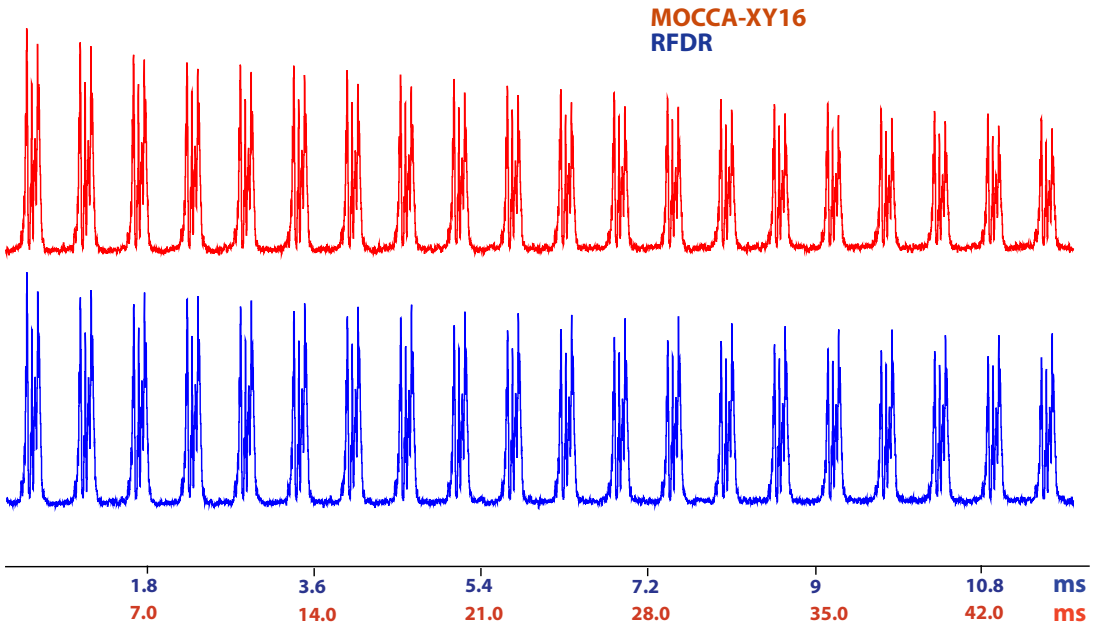

Fig. S5. 1D signal decays with increased number of loops for both RFDR (blue) and MOCCA (red). The scale of the mixing time for MOCCA and RFDR are shown in red and blue respectively.

Table S1. A list of the observed peaks and their ^{15}N, $^{1}H^{N}$, and ^{13}C chemical shift values of the α-spectrin SH3 domain.

Residue	^{15}N	^{1}HN	$^{13}C\alpha$	$^{13}C\beta$	$^{13}C\gamma$	$^{13}C\delta$	$^{13}C\varepsilon$
L8	120.3	7.7	53.3	45.6	26.3	23.6/22.6	
V9	111.0	8.8	58.1	36.1	24.2/21.1		
L10	123.8	8.9	53.3	46.6	25.5	25.0	
A11	127.6	9.1	52.9	19.3			
L12	127.6	9.1	56.4	42.9	26.5	22.3	
Y13	109.8	6.9	55.7	43.6			
D14	117.3	8.3	55.3	42.2			
Y15	118.7	8.5	60.8	43.5			
Q16	126.6	7.5	54.6	29.2	34.0		
E17	122	7.6	56.6	33.5	37.5		
K18							
S19	110.9	7.1	57.1	63.6			
P20			65.7	31.7	26.9	50.0	
R21							
E22	122.3	7.7	56.7	30.8	35.6		
V23	112.2	7.5	60.1	35.4	20.9/19.4		
T24	116.6	6.4	62.3	71.7	21.2		
M25	121.2	9.3	54.5	36.2	31.5		
K26	124.8	9.0	54.2				
K27	121.9	8.9	59				
G28	116.2	8.8	45.7				
D29	121.9	8.3	55.8	42.5			
I30	119.8	8.6	58.8	35.6	21.9/21.9	11.4	
L31	128.6	9.5	53.7	42.5	27.9	27.1/25.2	
T32	118.6	8.1	63.1	69.5	22.6		
L33	130	8.8	55.7	43	26.6/24.4		
L34	125.5	8.9	55.7	42.9	26.8	22.7	
N35	113.7	7.4	54.8	40.8			
S36	125	9.2	57.4	62.1			
T37	112.7	8.1	65.3	70.7	22.1		
N38	125.7	9.2	54.8	41.7			
K39	121.2	8.5	58.9				
D40	115.2	7.9	56.3	44.6			
W41	122.8	8.4	56.7	32.7			
W42	123.6	9.2	54.4	31.8			
K43	123.4	8.8	55.7	32.6	25.7		43.7
V44	121.8	9.4	59.7	37.1	21.5/19.1		
E45	119.8	8.8	55.4	33.8	37.7		
V46	125.5	8.8	60.7	33.4	20.4		
N47	129	7.4	54.8				
D48							
R49	118.8	8.0					
Q50	116.9	8.2	54.0	31.4			
G51	106.6	8.6	46.2				

F52	118.7	9.1	59.6	42.4				
V53	110.3	8.8	59	33.9	22.8/17.9			
P54			61.9	29.6	27.6	49.8		
A55	129	7.4						
A56	113.5	8.0	53.3	17.9				
Y57	113.1	7.2	55.3	37.4				
V58	110.6	7.3	58.6	35.8	22.8/20.0			
K59				36.4				42.2
K60								
L61	125.6	8.1	54.7	41.4	26.7	23.5		

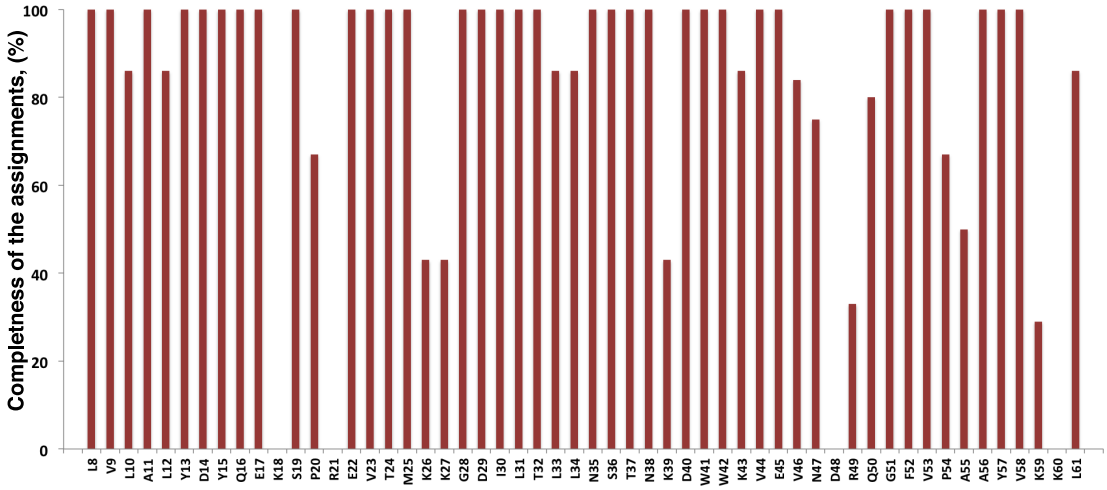

Fig. S6. Statistical analysis of the completeness of the side-chain assignments plotted in % as a function of the residue number. Here, we did not take aromatic side chain carbons into the consideration. For prolines, side-chain chemical shift information was taken from 2D ^{13}C-^{13}C correlation experiments.

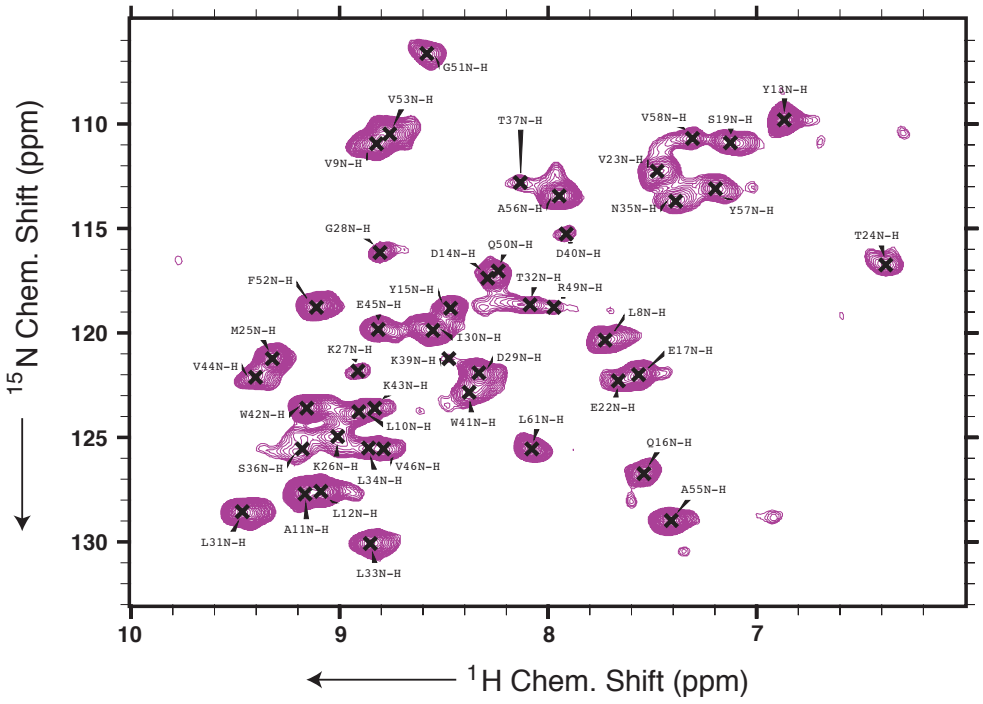

Fig. S7. First 2D plane of the 3D HCCCANH experiment performed on an 800 MHz spectrometer at 55.5 kHz spinning on the SH3 domain. The HN 2D plane represents the resolution with which the ^{13}C strips are dispersed in the 3D experiment.

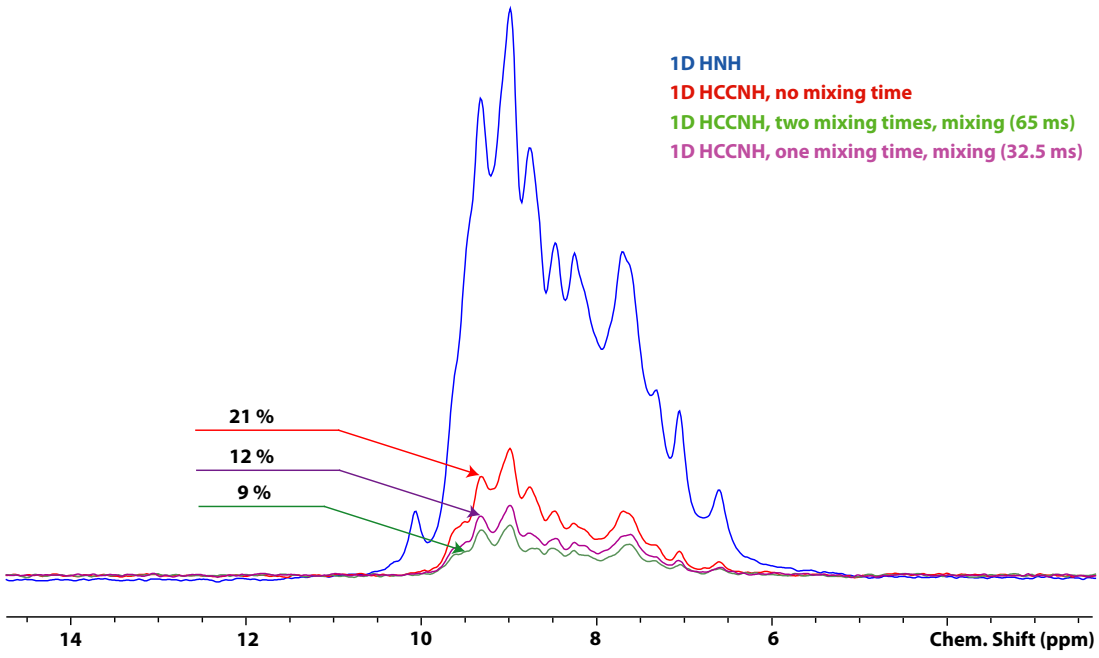

Fig. S8. Comparison of the first FID of the HNH (blue), (H)CX(CA)NH (denoted HCCNH here) without any mixing applied (red), with one mixing block in the sequence (purple, like in Fig. 1A of the main text) corresponding to a mixing time of 32.5 ms, and with two mixing blocks (green, like in Fig. 1B of the main text), using 65 ms of total mixing time considering the mixing before and after evolution period. Relative intensities are shown in %.

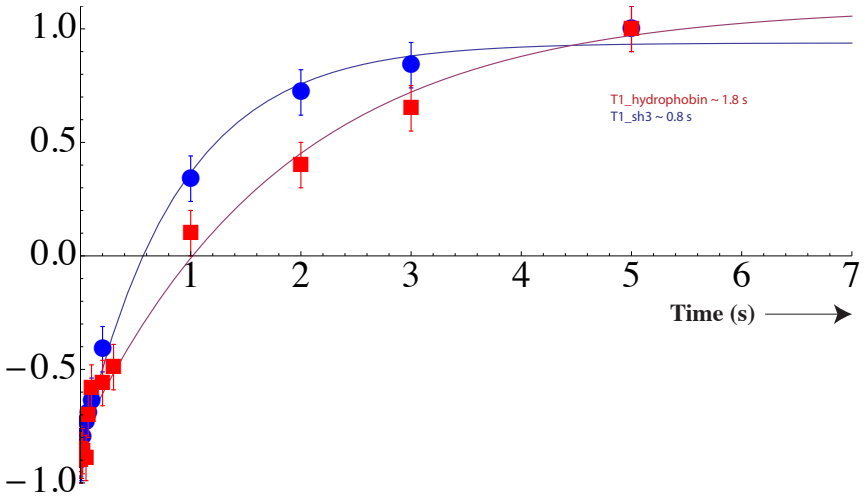

Fig. S9. ^{13}C T_1 inversion recovery data on the micro-crystalline SH3 domain in comparison with those on the hydrophobin rodlets. Hydrophobin rodlets, exposed to paramagnetic Cu-edta chelate after rodlet formation, show a higher aggregation level and an accordingly lower surface exposure. This weakens the paramagnetic doping effect, resulting in longer longitudinal relaxation times, despite identical dopant concentrations.

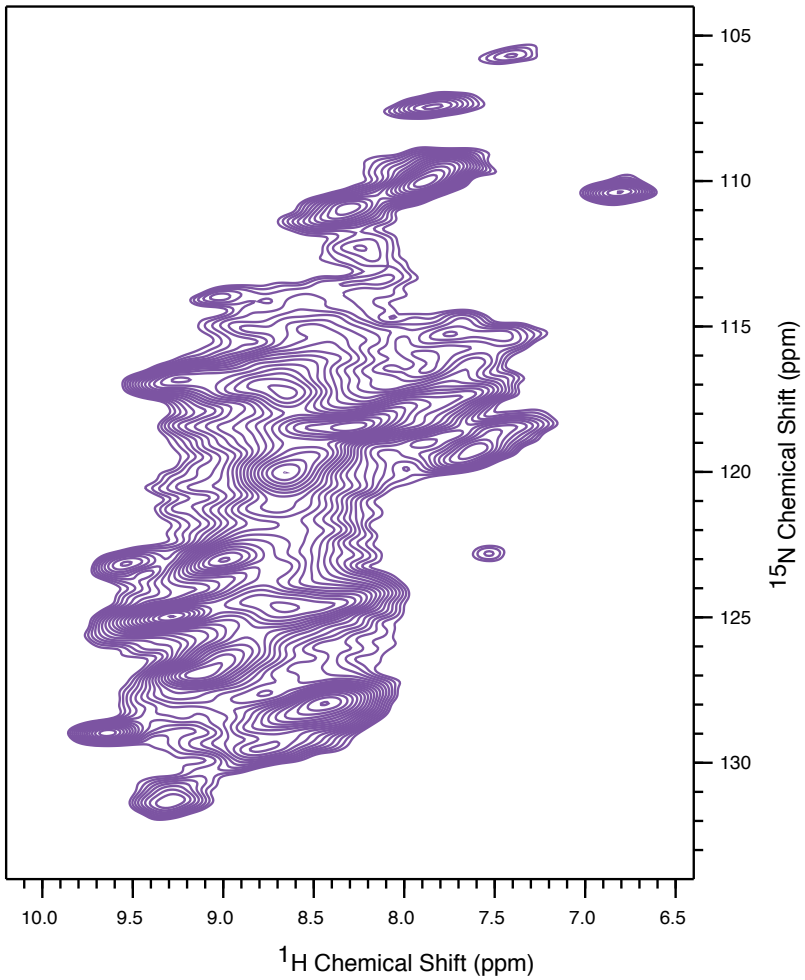

Fig. S10. The (H)NH 2D experiment performed on an 800 MHz spectrometer at 55.5 kHz spinning on the hydrophobin rodlets. Assignments and structural conclusions will be published elsewhere.

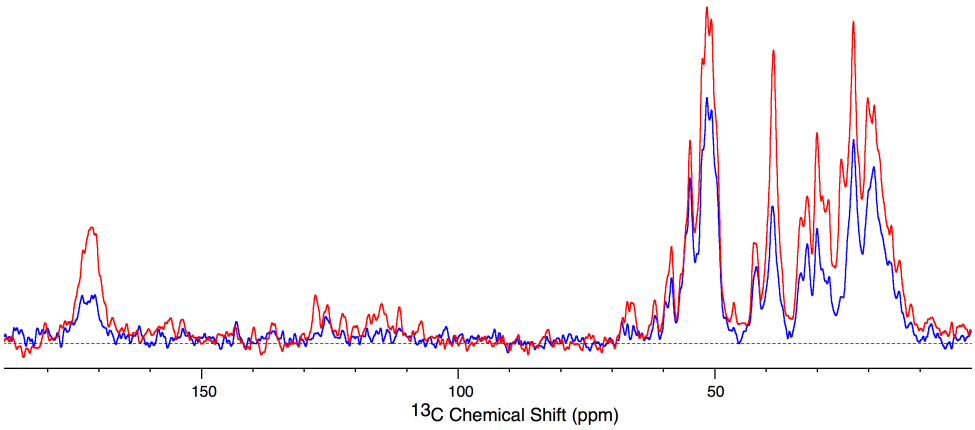

Fig. S11. A sensitivity comparison of ^{13}C cross-polarization (blue spectrum) experiment with the COPORADE[5] approach (red spectrum). Both experiments were acquired with similar experimental parameters with similar processing parameters on the SH3 domain sample. The fact that the methyl region is still quite intense even without the direct polarization component (CP spectrum) is due to the fact that this sample contains ILV methyl CH_3 labeling. The contact time for the cross-polarization step is 2.1 ms.

References:

1. K. H. Gardner, M. K. Rosen and L. E. Kay, *Biochemistry*, 1997, **36**, 1389-1401.
2. R. Linser, V. Chevelkov, A. Diehl and B. Reif, *J. Magn. Reson.*, 2007, 189, 209–216.
3. V. K. Morris, R. Linser, K. L. Wilde, A. P. Duff, M. Sunde and A. H. Kwan, *Angew Chem Int Edit*, 2012, 51, 12621-12625.
4. T. D. Goddard, D. G. Kneller, SPARKY 3, *University of California, San Francisco*.
5. R. Linser, *J. Biomol. NMR*, 2011, **51**, 221-226.